

CHAPTER 106

Numerical Study of Low Frequency Surf Zone Motions

H. Tuba Özkan-Haller¹ and James T. Kirby²

Abstract

This paper describes the application of a model of the two dimensional shallow water equations to the growth of instabilities of the longshore current at SUPERDUCK on October 18th. Simulations are carried out using two initial current profiles. In the first case the initial longshore current profile results from a balance between bottom friction, the radiation stress gradient and lateral mixing due to turbulence. In the second case lateral mixing is neglected. The shear wave climates resulting from both simulations are analyzed and compared to data. In the first case the energy in the shear wave band is underpredicted whereas in the second case, it is overpredicted. In both cases, the initial longshore current profile changes due to lateral mixing induced by the shear instabilities. The resulting longshore current profile after shear instabilities have reached finite amplitude is found to be very similar for both cases.

Introduction

Surf zone current measurements from experiments such as SUPERDUCK, Delilah, NSTS at Leadbetter beach, and others show that a variety of low frequency motions, such as edge waves, leaky waves, surf beat, rip currents and shear waves exist in the surf zone. These motions coexist and interact with each other as well as the short wave climate. Among these low frequency motions shear waves have been identified most recently. They were seen in current data from the SUPERDUCK experiment by Oltman-Shay *et al.* (1989) as a meandering of the longshore current over time scales up to $O(1000\text{ s})$. During the SUPERDUCK experiment a longshore array of current meters was positioned in the surf zone of a predominantly north-south tending beach at Duck, NC. A storm hit Duck on the 15th of October and caused a fairly stationary short wave field from the north quadrant through the 18th of October. During this four day period the shear wave climate was very energetic.

Time series of current measurements from one of the current meters in the surf zone for the 18th of October clearly show the meandering character of the

¹Graduate Student, Center for Applied Coastal Research, University of Delaware, Newark, DE 19716, USA. E-mail: ozkan@coastal.udel.edu

²Professor, Center for Applied Coastal Research, University of Delaware, Newark, DE 19716, USA.

In order to study these disturbances as they reach finite amplitude, a non-linear analysis needs to be employed. Such analyses were, to date, carried out by Dodd and Thornton (1992), Falqués *et al.* (1994), Özkan and Kirby (1995) and Allen *et al.* (1996). In these studies the spirit of a linear instability analysis is preserved since an initial current is generated and subsequently the temporal growth of the instabilities to finite amplitude is observed. In addition, Deigaard *et al.* (1994) performed a study where the longshore current was generated by ramping the short wave forcing. In their study the strengthening of the longshore current and the spatial growth of the instabilities were observed simultaneously.

In this study, we seek to find out whether or not instabilities of the longshore current are the source of the low frequency energy observed during the SUPER-DUCK experiment and to assess the importance of lateral mixing caused by shear instabilities. For this purpose we choose to simulate the low frequency climate on October 18th. Linear instability calculations for this day were previously carried out by Dodd *et al.* (1992) assuming straight and parallel bottom contours and a stationary wave field. Their results showed good agreement between the range of linearly unstable wavenumbers with observation as well as agreement between the linear prediction for the speed of propagation of the disturbances with observation.

Here, the analysis by Dodd *et al.* (1992) is taken one step further by carrying out a similar analysis using nonlinear computations. The assumption of straight and parallel bottom contours is retained, and it is also assumed that a stationary wave field forces an initial longshore current profile that subsequently becomes unstable. The instabilities are observed to grow to a finite amplitude and comparisons to data are made.

In the following, the governing equations of the model and their solution technique are discussed briefly. The generation of the initial longshore current profile is also documented along with results for the shear wave calculations and comparisons to data. For a detailed description of the numerical methods employed the reader is referred to Özkan-Haller and Kirby (1996a) where the application of the model to subharmonic edge waves is also documented.

Governing Equations

The governing equations are the nonlinear shallow water equations with added short wave forcing and bottom friction terms.

$$\begin{aligned}
 \frac{\partial \eta}{\partial t} + \frac{\partial}{\partial x}[u(h + \eta)] + \frac{\partial}{\partial y}[v(h + \eta)] &= 0 \\
 \frac{\partial u}{\partial t} + u \frac{\partial u}{\partial x} + v \frac{\partial u}{\partial y} &= -g \frac{\partial \eta}{\partial x} - \tau_{bx} \\
 \frac{\partial v}{\partial t} + u \frac{\partial v}{\partial x} + v \frac{\partial v}{\partial y} &= -g \frac{\partial \eta}{\partial y} + \tau_y - \tau_{vy}.
 \end{aligned} \tag{1}$$

Here, η is the water surface elevation above the mean water level, h is the depth with respect to the mean water level, u and v are the depth-averaged current velocities in the x and y directions, respectively, where x points offshore and y points in the longshore direction. The parameter τ_y represents the effect of the

short wave forcing in the y direction. The bottom friction is modeled using a linear representation assuming a small angle of wave incidence and weak mean longshore currents in relation to the horizontal wave orbital velocities, such that τ_{bx} and τ_{by} are given by

$$\tau_{bx} = \frac{\mu}{h + \eta} u, \quad \tau_{by} = \frac{\mu}{h + \eta} v, \quad (2)$$

where

$$\mu = \frac{2}{\pi} c_f u_0. \quad (3)$$

Here, u_0 is the horizontal orbital velocity of the short waves and can be expressed in terms of the wave height (Dodd *et al.*, 1992).

In order to estimate the term τ_y the short wave climate has to be considered. The bottom bathymetry at SUPERDUCK on October 18th is depicted in Figure 3a. It is characterized by a steep foreshore slope, a sand bar about 60 m offshore, and a milder offshore slope. The bathymetry on this day was fairly uniform in the longshore direction (Dodd *et al.*, 1992). The incident wave field measured at 8 m water depth consisted of waves from the north quadrant at about 15° to the beach inducing a southward longshore current. The root-mean-square (rms) wave height was about 1 m with a peak period around 5 sec.

In order to simulate the transformation of these random waves into shallow water, the wave height transformation model by Whitford (1988) which is based on Thornton and Guza (1983) is used. This model assumes random waves with Rayleigh distributed wave heights as well as wave stationarity and straight and parallel contours. The applicability of these assumptions to the SUPERDUCK experiment is discussed in Whitford (1988). The results of this model for the conditions on October 18th are given in Figure 3b. The waves are predicted to break at the seaward side of the bar, the breaking process stops at the shoreward side and strong breaking occurs on the foreshore slope.

Model Setup

The radiation stress gradient resulting from the short wave motion can now be computed. In the presence of this steady forcing and in the absence of any fluctuating motions a steady longshore current $V(x)$ would result, representing a balance between the radiation stress gradient, bottom shear stress, and lateral momentum mixing. The simplest formulation of the longshore balance neglects turbulent momentum exchange and incorporates a linearized bottom stress. The longshore current profile that would result from such a balance will have two peaks, one around the location of the bar crest and another close to the shoreline. This is due to the prediction that waves break as they approach the crest of the bar, cease to break as they travel into the trough region of the bar and break again on the shore. This mechanism causes two distinct areas of radiation stress forcing, hence the two peaks in the current which can be seen in Figure 3c.

In reality, however, significant currents are observed in the trough regions of barred profiles. A mixing mechanism is required to model such a case. The mixing can be due to many factors such as turbulent momentum mixing (Battjes,

1975), the contribution to the radiation stress by the rollers of breaking waves (Lippman *et al.*, 1995) and effects of depth variations of the nearshore currents (Svendsen and Putrevu, 1994). All of these mechanisms have the tendency to smooth the longshore current profile. As a simple but representative case of the effect of such mechanisms on the shape of the longshore current profile, turbulent momentum mixing is considered. The addition of a lateral mixing term (Battjes, 1975) into the mean longshore current balance decreases the magnitude of both peaks and introduces a significant current in the bar trough region. The current profile resulting from choosing a mixing coefficient of unity is depicted in Figure 3c and represents a good agreement with the current maximum as dictated by measurements. It should be noted that the amount of turbulent momentum mixing introduced here is unrealistically high, but it is anticipated that total mixing induced by the Taylor mixing process described by Svendsen and Putrevu (1994) added to a realistic treatment of turbulence and wave rollers is of comparable magnitude. A detailed discussion of the model and parameters used in obtaining these results can be found in Özkan-Haller and Kirby (1996b).

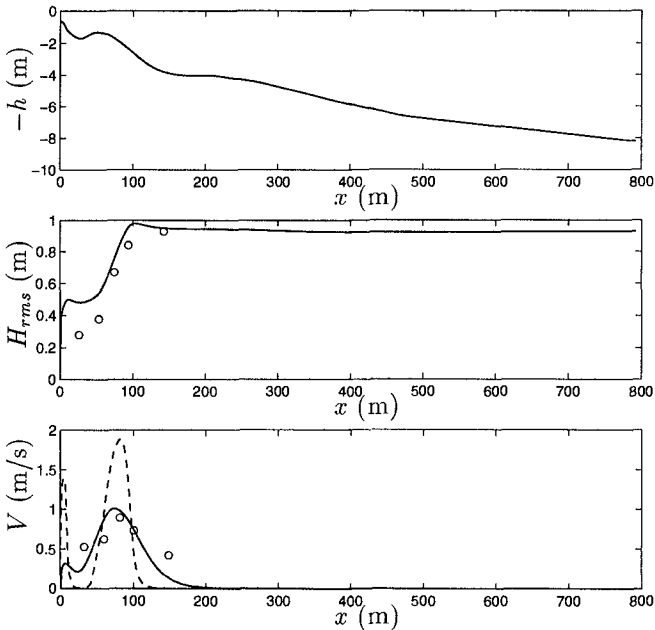


Figure 3: (a) Bottom bathymetry, (b) Wave height transformation, computed (solid) and measurements (o) and (c) Current profiles for October 18th, Case 1 (solid), Case 2 (dashed) and measurements (o).

The short wave forcing term in the y -momentum equation can now be expressed as

$$\tau_y = \frac{\mu}{h + \eta} V(x) \quad (4)$$

since the profile $V(x)$ is computed such that it is balanced with the steady

radiation stress gradient and the lateral mixing. Simulations with this forcing function result in the generation of the current $V(x)$ initially. It subsequently becomes unstable and finite amplitude shear instabilities develop.

In the following, two distinct initial current profiles will be used. The first case, hereafter referred to as Case 1, involves the initial current profile $V(x)$ depicted by the solid line in Figure 3c. In the second case, hereafter referred to as Case 2, any momentum mixing in the surf zone is neglected in the short wave forcing terms resulting in a $V(x)$ profile with two distinct peaks seen in Figure 3c (dashed line).

The shear wave climate for both of these forcing functions is computed for a given friction coefficient of $c_f=0.004$. This value has previously been used by Dodd *et al.* (1992). Linear instability analysis gives the wavenumber corresponding to the maximum growth rate in Case 1 as 0.0315 rad/m. The length of the modeling domain in the longshore direction L_y is chosen to be 16 times the wavelength that corresponds to this wavenumber. This longshore length scale is used in both cases since the most unstable wavenumber for Case 2 occurs at higher wavenumbers due to the presence of the highly unstable shoreline jet. The modeling domain extends 400 m offshore. An absorbing boundary condition is used at the offshore boundary (Özkan-Haller and Kirby, 1996a). Periodicity is assumed in the longshore direction. The current profile $V(x)$ corresponding to the each case is specified as an initial condition.

Results for Case 1

The simulation for the forcing profile including the effects of additional mixing is presented first. Time series taken in the trough region of the bar (about 35 m offshore) are shown in Figure 4. The longshore averaged longshore velocity is also shown and is defined as

$$\bar{v}(x, t) = \frac{1}{L_y} \int_0^{L_y} v(x, y, t) dy. \quad (5)$$

It can be observed that the instabilities gain energy about one hour into the simulation, the time series display an intermittent character where periods of higher frequency oscillations are followed by periods of low frequency oscillations. A mean longshore current already exists in the trough region; it is seen to increase slightly after the shear instabilities reach finite amplitude.

The intermittent character of the motion is also evidenced by plots of the potential vorticity defined as

$$q = \frac{v_x - u_y}{h + \eta}. \quad (6)$$

The patterns of potential vorticity shown in Figure 5 are propagating in the $+y$ direction and show that features with longer longshore scales are followed by packets of features with shorter longshore scales.

To aid the interpretation of the potential vorticity a plot of the circulation pattern in a portion of the domain depicted in Figure 5 is shown in Figure 6a. The shear instabilities can be observed to cause flow across the bar crest which is located about 60 m offshore. Also of interest are the offshore directed velocities

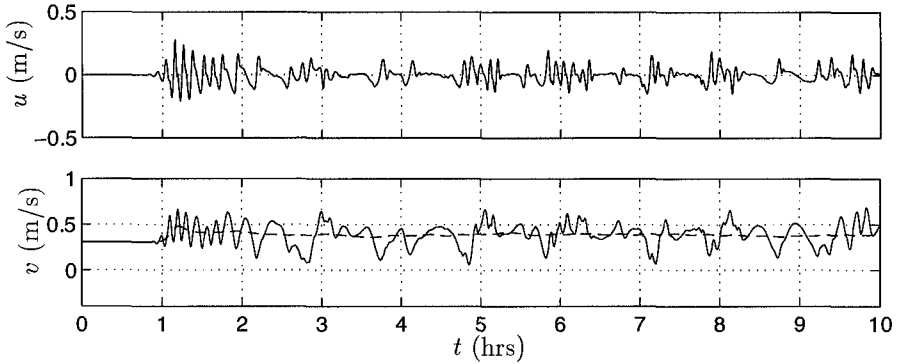


Figure 4: **Case 1** Time series of u and v in the bar trough region (solid) and longshore averaged longshore velocity \bar{v} (dashed).

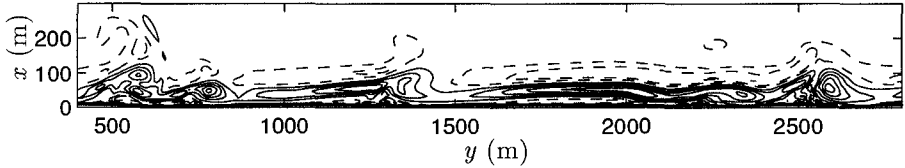


Figure 5: **Case 1** Contour plot of potential vorticity (solid for $q > 0$, dashed for $q < 0$) at $t=10$ hrs.

occurring further offshore. These features can be seen to be active up to about 250 m offshore corresponding to about 3 times the surf zone width.

The change in the mean longshore current profile that occurs as the shear instabilities reach finite amplitude is documented in Figure 7a where the initial current profile is shown along with the mean current profile after the instabilities develop. It can be noted that the value of the current maximum as well as the value of its slope on the seaward side have decreased. Multiplying the longshore momentum equation (1) by the total water depth, longshore averaging, and assuming stationarity of the mean quantities identifies the dominant terms and leads to a balance between lateral mixing induced by the shear instabilities and the change in the mean longshore current profile given by

$$\overline{(Duv)_x} = -\mu(\bar{v} - V), \quad (7)$$

where subscripts denote differentiation and $D = h + \eta$ is the total water depth. The initial current profile is denoted by V and \bar{v} is the current profile after the development of the shear instabilities. Any change in the longshore current profile is, therefore, directly due to lateral momentum mixing induced by the shear instabilities.

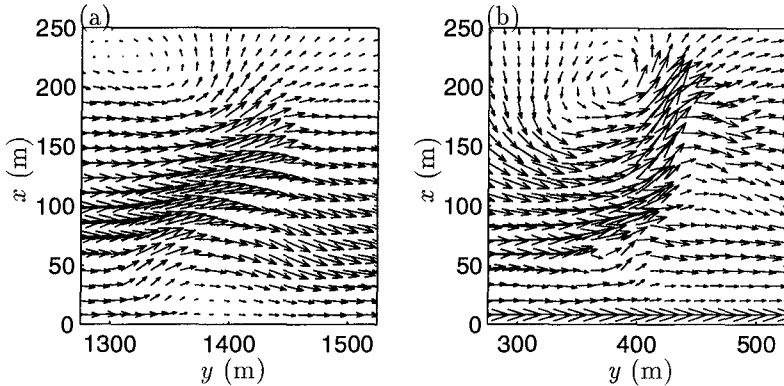


Figure 6: Circulation pattern at $t=10$ hrs (a) Case 1 (b) Case 2.

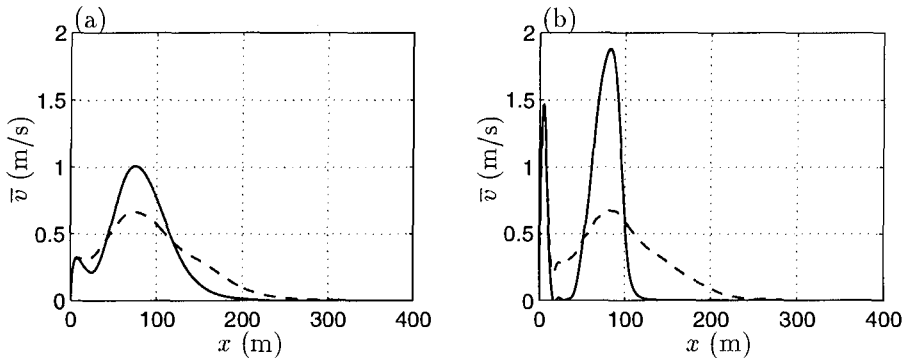


Figure 7: Initial (solid) and final (dashed) mean current profiles (a) Case 1 (b) Case 2.

Results for Case 2

Results for the simulation involving the forcing function with no mixing involved are discussed next. Time series for the velocity components (see Figure 8) show that the instabilities reach finite amplitude in a shorter amount of time than in Case 1. Higher frequency oscillations are evident but there is no evidence of intermittent behavior. It can be noted that there is no mean current at this location initially but a mean current of about the same magnitude as in Case 1 is created after the instabilities reach finite amplitude. The oscillations also appear to be more energetic in this case.

A contour plot of the potential vorticity at the end of the simulation (see Figure 9) shows that the organized layers of positive and negative potential vorticity are being mixed. Features with positive and negative potential vorticity can be seen to pair up. Some pairs that have previously been released are seen about 300 m offshore. The resulting pattern is similar to results obtained by

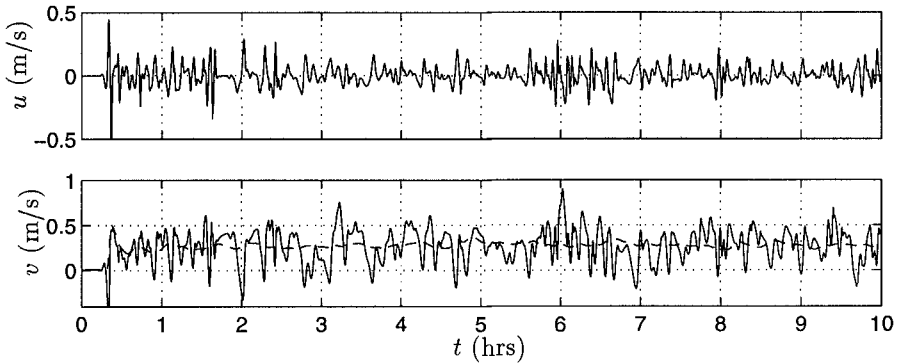


Figure 8: **Case 2** Time series of u and v in the bar trough region (solid) and longshore averaged longshore velocity \bar{v} (dashed).

Slinn *et al.* (1995) for a generic barred beach in a regime they called “eddy formation”.

An interesting feature can be seen in Figure 9 around $y = 400$ m. It resembles a “rip-head”. A plot of the circulation pattern associated with this feature is given in Figure 6b and exhibits strong offshore directed velocities across the bar crest extending offshore, much like a rip current. Flow across the bar trough is also evident.

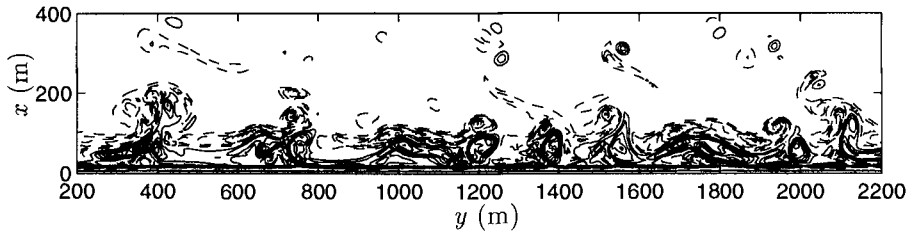


Figure 9: **Case 2** Contour plot of potential vorticity (solid for $q > 0$, dashed for $q < 0$) at $t=10$ hrs

The change in the mean longshore current profile due to the shear instabilities can be observed in Figure 7b. The peak longshore current has decreased significantly due to the presence of the shear waves. In addition, an appreciable current is introduced in the trough region of the bar.

Comparisons with data

The predictions for the final mean longshore current for the two cases are plotted in Figure 10 along with data points from sequential measurements from a measurement sled that was pulled onshore during an experimental run, collecting data for 35 minutes at each stop. It should be noted that the current profiles

resulting from the two cases are remarkably similar. They exhibit similar maximum current values, the seaward slope of the current profiles are also similar. However, the current profile resulting from simulations for Case 2 shows a strong shoreline jet. The maximum longshore current is underpredicted by about 20 %. However, caution should be used in interpreting the data to model agreement in this case since the measurements were carried out sequentially and sled data and model data are based on very different averaging periods.

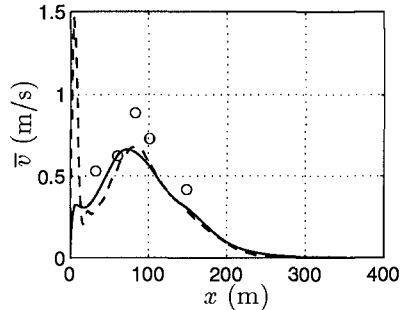


Figure 10: Final mean current profiles for Case 1 (solid) and Case 2 (dashed), measurements (o)

Time series obtained from the model can be compared to velocity measurements from one of the current meters located in the surf zone. Three hour segments of computations for the two cases as well as measurements of cross-shore and longshore velocities are shown in Figure 11. The time scales involved in Case 1 are much longer than what is seen in the data. The intermittent character is also not repeated in the data. In turn, simulations for Case 2 exhibit more high frequency activity than Case 1, but the fluctuations have higher amplitudes than the fluctuations seen in the data.

Frequency spectra for the longshore velocities confirm that the energy in high frequencies is underpredicted in Case 1 (see Figure 12a). The shape of the spectrum in Case 2 (see Figure 12b) is similar to that of data but the energy in the motions is overpredicted. The same trend can be seen in frequency spectra of the cross-shore velocities shown in Figure 13.

In order to determine if the propagation speeds of these motions are predicted well, comparisons of frequency-longshore wavenumber spectra for the longshore velocities are made. Frequency-longshore wavenumber spectra are obtained using the high resolution Iterative Maximum Likelihood Estimator (IMLE) utilizing time series from five sensors in the surf zone (Oltman-Shay *et al.*, 1989) (see Figure 14a). Since model computations are carried out with high resolution in both space and time a direct Fourier Transform in both space and time is used to obtain the two-dimensional spectra from the computed time series (see Figure 14b and c).

Results for Case 1 show that the wavenumber range in which shear instabilities are present is underpredicted as is expected after analyzing frequency spectra. The predicted spectra displays a nondispersive character. The two-dimensional spectra for Case 2 predicts a wider range of wavenumbers where

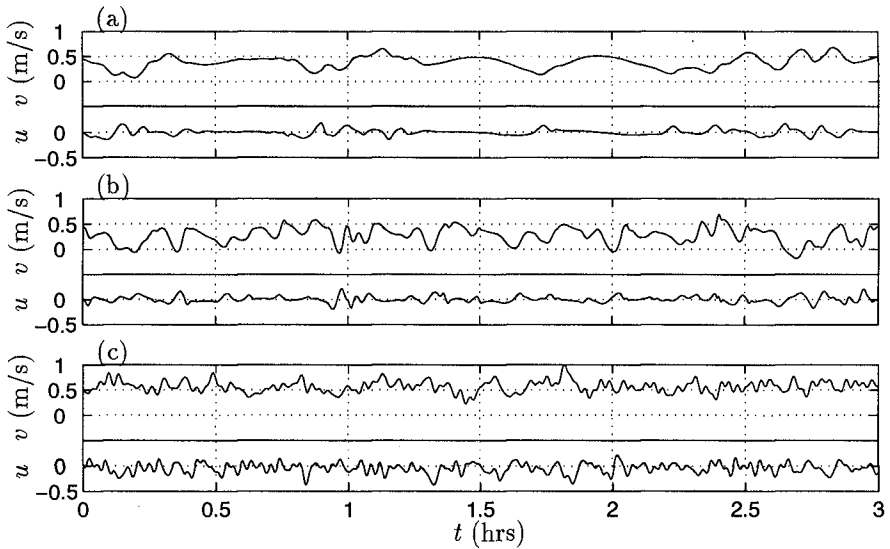


Figure 11: Three hour segments of time series (a) Case 1 (b) Case 2 (c) Data from gage LS07 at SUPERDUCK, October 18th.

shear instabilities are present. The slight increase in the speeds with increasing frequency is also reproduced. The propagation speeds are similar in both cases and correspond to an underprediction of the propagation speed seen in the data by about 20 %. This is likely to be a direct consequence of the fact that the peak mean longshore current velocity is underpredicted by about 20 %, since the shear instabilities propagate at a fraction of the maximum mean longshore current velocity (Bowen and Holman, 1989).

Summary and Conclusions

In this study, a comprehensive model of low frequency motions has been used to study the shear wave climate on October 18th at SUPERDUCK. Two cases including and neglecting a simple lateral mixing mechanism, respectively, are simulated. Time series, frequency spectra, frequency-longshore wavenumber spectra and time variations of the mean longshore current profiles are analyzed for both cases, the results are compared to measurements where possible.

It is seen that when intensive mixing is considered in the forcing function (Case 1) the mean current profile only changes slightly, therefore the lateral mixing caused by the shear instabilities is small. The resulting shear wave climate is not very energetic, underpredicting what is seen in data. In turn, if mixing due to mechanisms related to the short wave climate and turbulence is neglected entirely in the forcing function (Case 2), the initial profile undergoes drastic changes, therefore lateral mixing induced by the shear instabilities is appreciable and the shear wave climate is very energetic, overpredicting what is seen in data. The final longshore current profiles resulting from the simulations

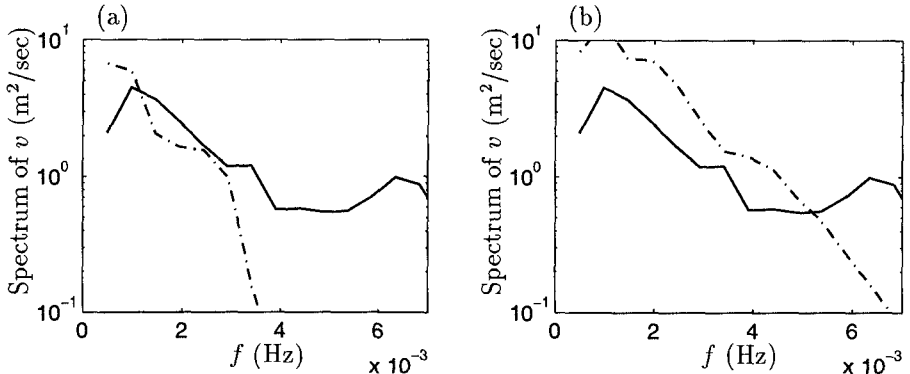


Figure 12: Frequency spectra for v , measured (solid), computed (dashed-dotted) (a) Case 1 (b) Case 2.

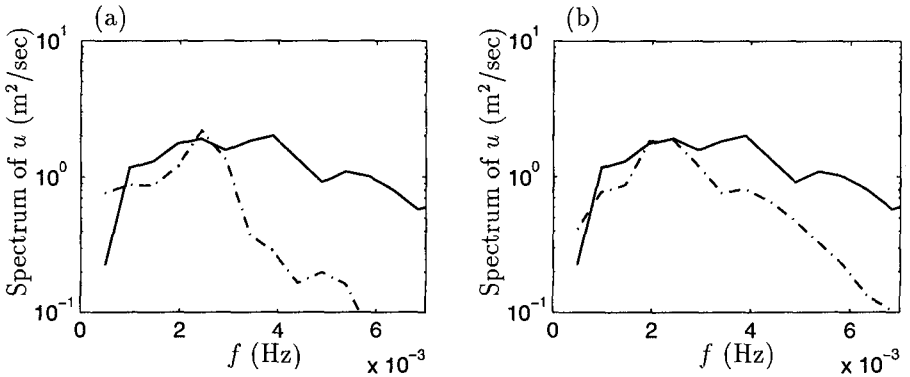


Figure 13: Frequency spectra for u , measured (solid), computed (dashed-dotted) (a) Case 1 (b) Case 2.

are remarkably similar regardless of the shape of the initial current profile. If the short wave forcing is far removed from producing this final current profile, shear instabilities arise, causing enough lateral mixing to redistribute the momentum in the surf zone.

In conclusion, the results of this study suggest that in this model the final mean longshore current profile is not a function of how much lateral mixing is initially included into the model, but only a function of the friction factor. If no (intensive) mixing due to the turbulence or Taylor dispersion is initially considered, the shear wave climate responds by creating intensive (minimal) mixing. Therefore, in this model the amount of energy in the shear wave band is a function of how much lateral mixing due to other considerations is already present in the initial forcing function. Hence, it is anticipated that the accurate prediction of the amount of energy present in the shear wave band in data is strongly linked to an accurate representation of the mixing processes due to turbulence, depth variations in the current or additional physics in the breaking process.

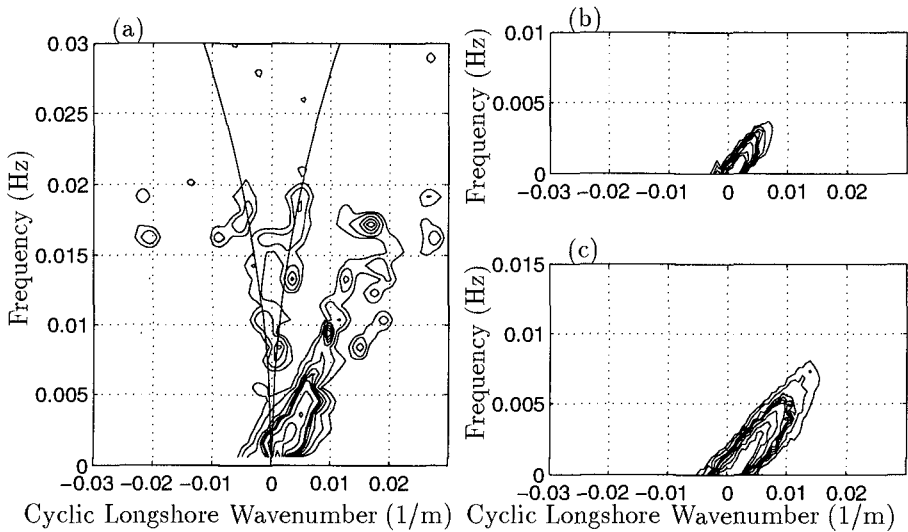


Figure 14: Frequency-longshore wavenumber spectrum for the longshore velocity v (a) Data for October 18th (b) Case 1 (c) Case 2.

Acknowledgments. The authors thank Dr. U. Putrevu for providing the software used to carry out linear instability calculations. Thanks are also due to Dr. J. Oltman-Shay for providing the SUPERDUCK data as well as the software to obtain estimates for two-dimensional spectra of the data. Thanks also to Dr. N. Dodd for providing the measured depth profiles used herein. This research has been sponsored by the Office of Naval Research, Coastal Sciences Program.

References

- Allen, J., P.A. Newberger and R.A. Holman (1996). "Nonlinear shear instabilities of alongshore currents on plane beaches." *J. Fluid Mech.*, 310, 181-213.
- Battjes, J. (1975). "Modeling of turbulence in the surf zone." *Proc. Symposium on Modeling Techniques*, San Francisco, 1050-1061.
- Bowen, A.J. and R.A. Holman (1989). "Shear instabilities of the mean longshore current. 1. Theory." *J. Geophys. Res.*, 94, 18023-18030.
- Deigaard, R., E.D. Christensen, J.S. Damgaard and J. Fredsøe (1994). "Numerical simulation of finite amplitude shear waves and sediment transport." *Proc. 24th Intl. Conf. Coastal Eng.*, Kobe, 1919-1933.
- Dodd, N. (1994). "On the destabilization of a longshore current on a plane beach: Bottom shear stress, critical conditions, and onset of stability." *J. Geophys. Res.*, 99, 811-824.

- Dodd, N., and E.B. Thornton (1990). "Growth and energetics of shear waves in the nearshore." *J. Geophys. Res.*, 95, 16075-16083.
- Dodd, N. and E.B. Thornton (1992). "Longshore current instabilities: Growth to finite amplitude." *Proc. 23rd Intl. Conf. Coastal Eng.*, Venice, 2655-2668.
- Dodd, N., J. Oltman-Shay and E.B. Thornton (1992). "Shear instabilities in the longshore current: A comparison of observation and theory." *J. Phys. Oceanog.*, 22, 1, 62-82.
- Falqués, A. and V. Iranzo (1994). "Numerical simulation of vorticity waves in the nearshore." *J. Geophys. Res.*, 99, 825-841.
- Falqués, A., V. Iranzo and M. Caballería (1994). "Shear instability of longshore currents: Effects of dissipation and nonlinearity." *Proc. 24th Intl. Conf. Coastal Eng.*, Kobe, 1983-1997.
- Lippman, T.C., E.B. Thornton and A.J.H.M. Reniers (1995). "Wave stress and longshore current on barred profiles." *Proceedings of Coastal Dynamics 1995*, Gdansk, Poland, 401-412.
- Oltman-Shay, J., P.A. Howd and W.A. Birkemeier (1989). "Shear instabilities of the mean longshore current. 2. Field Observation." *J. Geophys. Res.*, 94, 18031-18042.
- Özkan, H.T. and J.T. Kirby (1995). "Finite amplitude shear wave instabilities." *Proceedings of Coastal Dynamics 1995*, Gdansk, Poland, 465-476.
- Özkan-Haller, H.T. and J.T. Kirby (1996a). "A Fourier-Chebyshev collocation method for the shallow water equations including shoreline runup." *Appl. Ocean Res.*, in press.
- Özkan-Haller, H.T. and J.T. Kirby (1996b). "Shear instabilities of the longshore current on a barred beach: A comparison of observation and nonlinear computations." in preparation.
- Putrevu, U. and I.A. Svendsen (1992). "Shear instability of longshore currents: A numerical study." *J. Geophys. Res.*, 97, 7283-7303.
- Slinn, D.N., J.S. Allen and R.A. Holman (1995). "Nonlinear shear instabilities of alongshore currents over barred beaches." *AGU Fall Meeting, 1995*, San Francisco, CA.
- Svendsen, I.A. and U. Putrevu (1994). "Nearshore mixing and dispersion." *Proc. Roy. Soc. Lond. A*, 445, 561-576.
- Thornton, E.B. and R.T. Guza (1983). "Transformation of wave height distribution." *J. Geophys. Res.*, 88, 5925-5938.
- Whitford, D.J. (1988). "Wind and wave forcing of longshore currents across a barred beach." Ph.D. Dissertation, Naval Postgraduate School, pp. 202.